JPE 16-4-35

http://dx.doi.org/10.6113/JPE.2016.16.4.1621
ISSN(Print): 1598-2092 / ISSN(Online): 2093-4718

A Topological Transformation and Hierarchical Compensation Capacitor Control in Segmented On-road Charging System for Electrical Vehicles

Han Liu*, Linlin Tan*, Xueliang Huang†, Jinpeng Guo*, Changxin Yan*, and Wei Wang*

*,†School of Electrical Engineering, Southeast University, Nanjing, China

Abstract

Experiencing power declines when the secondary coil is at the middle position between two primary coils is a serious problem in segmented on-road charging systems with a single energized segmented primary coil. In this paper, the topological transformation of a primary circuit and a hierarchical compensation capacitor control are proposed. Firstly, the corresponding compensation capacitors and receiving powers of different primary structures are deduced under the condition of a fixed frequency. Then the receiving power characteristics as a function of the position variations in systems with a single energized segmented primary coil and those with double segmented primary coils are analyzed comparatively. A topological transformation of the primary circuit and hierarchical compensation capacitor control are further introduced to solve the foregoing problem. Finally, an experimental prototype with the proposed topological transformation and hierarchical compensation capacitor control is carried out. Measured results show that the receiving power is a lot more stable in the movement of the secondary coil. It is a remarkable fact that the receiving power rises from 10.8W to 19.2W at the middle position between the two primary coils. The experimental are in agreement with the theoretical analysis.

Key words: Hierarchical compensation capacitor control, Receiving power, Segmented on-road charging, Topological transformation

I. INTRODUCTION

Electrical vehicles (EVs) are being liberated from cable charging with wireless power transfer technology, which reduces the chances of electric shocks. There have been attempts to apply wireless power transfer technology in static EVs charging systems [1]-[6]. Researches with respect to this field focus on the design of the high frequency inverter [3], [4], the optimization design of the resonators [3], [5] and the system structures [6]. In order to resolve existing problems such as the low energy density of the battery, frequent charging and high cost due to a heavy battery, on-road charging for EVs has been proposed [7]-[9]. If EVs can be powered while driving, battery capacity can be reduced quite a lot. Studies of on-road charging for EVs are reviewed in [7]. The schemes of the power supply are divided into two categories by considering the structures of the transmitting rail. One is a charging rail composed of long transmitting coils [9]-[14], while the other is a segmented charging structure including several short primary coils [8], [15]-[21].

Discussions of structures with long transmitting coils focus on the design of the transmitting devices [9]-[11], novel modeling methods [12] and the elimination of electromagnetic radiation [13]. [14]. Comparatively, segmented charging structure with short primary coils should rely on the real-time position detection of EVs [15] and the necessary switches to control the on and off switching of the primary circuits [8]. However, it also has the advantages of lower loss on the primary side, lower power requirements for the power sources and a more secure electromagnetic environment. In [16], the response time of a typical on-road charging system is investigated to determine the moment of turning on for the next primary coil. In [17], a compensation circuit is designed to reduce the losses of an inverter when all of the transmitting coils are powered. In [18], switches to turn on and off the

Manuscript receive Jan. 11, 2016; accepted Mar. 14, 2016
Recommended for publication by Associate Editor Jee-Hoon Jung.
†Corresponding Author: xlhuang@seu.edu.cn
Tel: +86-025-83794691, Southeast University
*School of Electrical Engineering, Southeast University, China

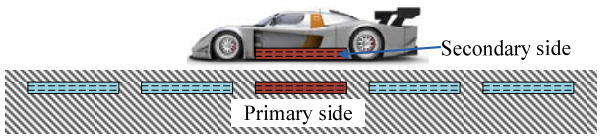

Fig. 1. Diagram of on-road charging system with short segmented primary coils.

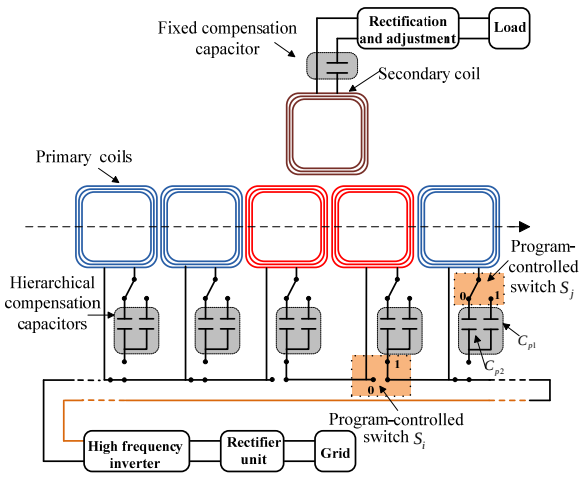

Fig. 2. Structure schematic of on-road charging system.

segmented transmitting coils play the role of invertors to transform DC to AC with a high frequency. In [19], power fluctuations are discovered in an on-road charging system composed of segmented circular primary coils when the secondary coil is moving. In [20], the challenges and development trends of on-road charging for EVs are summarized.

In wireless power transfer systems, misalignment between the primary side and the secondary side results in a decline in the receiving power and power transfer efficiency. The misalignment issues in on-line charging systems can be divided into lateral misalignment and longitudinal misalignment. The main researches focus on solving the lateral misalignment issue. In [21]-[24], the researchers focused on the design of transmitting coil structures with a high lateral misalignment tolerance. As for the longitudinal misalignment issue, power fluctuations have been discovered in an on-road charging system composed of segmented circular primary coils while the secondary coil is moving in [19]. Lateral misalignment can be avoided by setting routing instructions and intelligent drive. Therefore, this paper focuses on reducing the power fluctuations caused by the secondary coil's longitudinal movement.

If segmented charging structure is used in on-road charging systems, one concerning issue is dealing with power fluctuations. On one hand, the receiving power decreases when the secondary coil is in the middle position of two primary coils if only one primary coil is energized at a time. On the other hand, there will be more power loss if all of the primary coils in the segment are energized [17]. As a result, the

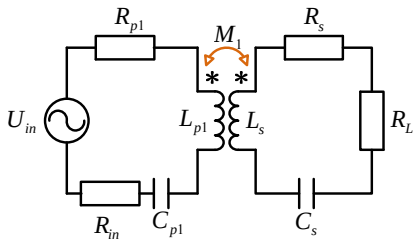

Fig. 3. Equivalent circuit of system with single primary coil topology.

topology transform of the primary transmitting coils and the compensation capacitor control are proposed in this paper to maintain a high receiving power without a frequency adjustment. Finally, experimental verification is carried out to demonstrate the correctness of the theoretical analysis.

II. Proposed Segmented On-road Charging System

Short segmented primary coils buried under the ground can power moving EVs by electromagnetic coupling with the secondary coil installed under the chassis of EVs, as shown in Fig. 1.

A typical on-road charging system includes a high frequency inverter, square primary coils, a hierarchical compensation capacitor on the primary side, program-controlled switches, a square secondary coil, a fixed compensation capacitor on the secondary side, a rectifier, a voltage regulator and a load. As shown in Fig. 2, the primary coil is controlled by the corresponding program-controlled switch. The coil is turned on when S_i=1 and turned off when S_i=0 . The hierarchical compensation capacitors are controlled by a programmed switch S_j . Specifically, capacitor C_{p1} is adopted to compensate for the single primary coil topology when S_j=1 and capacitor C_{p2} is adopted to compensate for the two primary coil topology when S_j=0 .

III. System Modeling and Analysis

The equivalent circuit of a system with a single primary coil topology is shown in Fig. 3. Both the primary and secondary sides are connected in series. U_{in} represents the power source voltage. R_{in} is the inner resistance of the power source. f and ω denote power frequency and angular frequency, respectively, and they comply with $\omega = 2\pi f$. R_L is the load resistance. R_{p1} and L_{p1} are used to represent the inner resistance and inductance of primary coil 1. R_s and L_s are used to denote the inner resistance and inductance of the secondary coil. C_s stands for the fixed compensation capacitor on the secondary

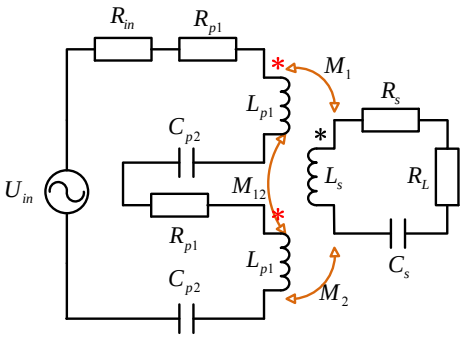

Fig. 4. Equivalent circuit of system with two primary coils topology.

side. The mutual inductance between primary coil 1 and the secondary coil is indicated by M_1. The parameters of the primary coils and the secondary coil are the same so that $R = R_{p1} = R_s$ and $L = L_{p1} = L_s$.

Hence, based on the mutual inductance theory, systems with a single primary coil topology can be modeled with the following voltage equations:

$$U_{in} = \left(R_{in} + R_{p1} + j\omega L_{p1} + \frac{1}{j\omega C_{p1}} \right) I_{p1} + j\omega M_1 I_{s1} \quad (1)$$

$$0 = j\omega M_1 I_{p1} + \left(R_s + j\omega L_s + \frac{1}{j\omega C_s} + R_L \right) I_{s1} \quad (2)$$

Where I_{p1} represents current in the primary side, and I_{s1} is current in the secondary side.

If the system resonant frequency is equal to the power frequency, C_{p1} can be expressed by:

$$C_{p1} = \frac{1}{\omega^2 L} \quad (3)$$

By solving voltage equations (1) and (2), the receiving power can then be calculated by:

$$P_1 = \frac{\omega^2 M_1^2 U_{in}^2 R_L}{\left\{ \left(R_L + R \right) \left(R + R_{in} \right) + \omega^2 M_1^2 \right\}^2} \quad (4)$$

Systems with two primary coils are obtained by adding another coil referred to as primary coil 2 with same parameters. Primary coil 2 connects with primary coil 1 in series, as shown in Fig. 4. M_2 represents the mutual inductance between primary coil 2 and the secondary coil. M_{12} denotes the mutual inductance between primary coil 1 and primary coil 2.

For the same reason, based on the mutual inductance theory, systems with a two primary coil topology can be modeled with the following voltage equations:

$$U_{in} = \left(R_{in} + Z_{p1} + Z_{p2} + 2\, j\omega M_{12} \right) I_{p2} + j\omega \left(M_1 + M_2 \right) I_{s2} \quad (5)$$

$$0 = j\omega \left(M_1 + M_2 \right) I_{p2} + \left(R_s + j\omega L_s + \frac{1}{j\omega C_s} + R_L \right) I_{s2} \quad (6)$$

Where the equivalent impedances of the primary resonant cavities are derived as $Z_{p1} = R_{p1} + j\omega L_{p1} + \frac{1}{j\omega C_{p1}}$ and $Z_{p2} = R_{p2} + j\omega L_{p2} + \frac{1}{j\omega C_{p2}}$ respectively, where I_{p2} represents the current in the primary side, and I_{s2} is the current in the secondary side.

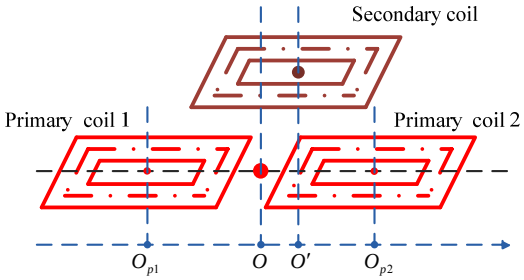

Fig. 5. Diagram of primary and secondary coils.

According to (5), to guarantee a resonant working status, the primary capacitors should compensate for the inductor equal to $L_{sum} = 2L + 2M_{12}$. Since $\omega = \frac{1}{\sqrt{\frac{L_{sum} C_{p2}}{2}}}$, C_{p2} can be calculated by:

$$C_{p2} = \frac{1}{\omega^2 \left(L + M_{12} \right)} \quad (7)$$

By solving voltage equations (5) and (6), the output power can then be calculated by:

$$P_2 = \frac{\omega^2 \left(M_1 + M_2 \right)^2 U_{in}^2 R_L}{\left\{ \left(R_L + R \right) \left(2R + R_{in} \right) + \omega^2 \left(M_1 + M_2 \right)^2 \right\}^2} \quad (8)$$

Comparing (3) with (7), when the coil inductance L and the working angular frequency ω are fixed, C_{p1} is a constant while C_{p2} is determined by M_{12}.

As shown in Fig. 5, the secondary coil moves in a horizontal direction. O refers to the middle position of the two primary coils. O' represents the position of the secondary coil. O_{p1} and O_{p2} denote the positions of coil 1 and coil 2, respectively. When the secondary coil moves to a position right above coil 1 (O' overlaps with O_{p1}), the secondary coil is far away from primary coil 2 leading to a small M_2. As a result, $M_1 + M_2 \approx M_1$. In addition, it is observed that systems with two primary coils have a larger primary resistance. On the basis of (4) and (8), it can be derived that $P_1 > P_2$.

When the secondary coil moves to the middle position of the two primary coils, O' overlaps with O_{p1}. At this point, for systems with a single primary coil topology, M_1 decreases in accordance to a large misalignment. As a result, P_1 declines.

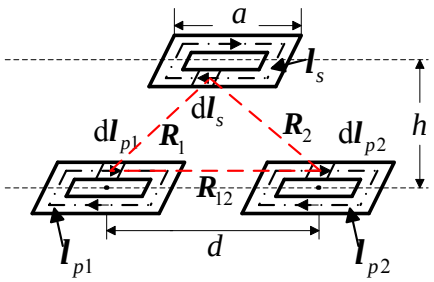

Fig. 6. Sketch map for mutual inductance calculation.

However, for systems with a two primary coils topology, the mutual inductance is increased to twice by a series connection of the primary coils. However, the primary coils inner resistance is also increased to twice. The effect of the increased primary coils inner resistance on the power is negligible compared with that of the power source inner resistance. Under this circumstance, it is obvious that $P_1 < P_2$.

To sum up, when the secondary coil (O') moves from O_{p1} to O, the size relationship between the receiving powers of the two topologies changes from $P_1 > P_2$ to $P_1 < P_2$. When the secondary coil (O') moves from O to O_{p2}, the size relationship between the receiving powers of the two topologies changes from $P_1 < P_2$ to $P_1 > P_2$. As a result, the two positions between O_{p1} and O_{p2} can be determined where $P_1 = P_2$.

In order to accurately obtain the critical positions, assume (4) is equal to (8). According to (4) and (8), the condition where $P_1 = P_2$ can be generated by:

$$\omega^2 M_1 M_2 (M_1 + M_2) + (R_L + R)(RM_1 - RM_2 - R_{in}M_2) = 0 \quad (9)$$

The critical positions are where the mutual inductances meet equation (9) in the process of the secondary coil's movement. The mutual inductances in the receiving power and condition formulas can be calculated by the following analysis. Fig. 6 depicts the *N*-turns square coil, made by a thin copper wire, used for both the primary and secondary coils. A constant *a* denotes the width of the coil and a constant *h* represents the air gap between the primary coil and the secondary coil. Then based on Neumann's formula, the mutual inductance between each of the primary coils and secondary coil can be indicated as:

$$M_i = \frac{N^2 \mu_r \mu_0}{4\pi} \oint_{l_{pi}} \oint_{l_s} \frac{d\boldsymbol{l}_{pi} d\boldsymbol{l}_s}{\boldsymbol{R}_i}, \quad i = 1, 2. \quad (10)$$

In addition, the mutual inductance between the two primary coils can be expressed as:

$$M_{12} = \frac{N^2 \mu_r \mu_0}{4\pi} \oint_{l_{p1}} \oint_{l_{p2}} \frac{d\boldsymbol{l}_{p1} d\boldsymbol{l}_{p2}}{\boldsymbol{R}_{12}} \quad (11)$$

where μ_r denotes the relative permeability, μ_0 means the permeability of vacuum, $\boldsymbol{l}_{pi}$ represents the directed loop in the primary coil *i*, and $\boldsymbol{l}_s$ represents the directed loop in the secondary coil. Additionally, $d\boldsymbol{l}_{p1}$, $d\boldsymbol{l}_{p2}$ and $d\boldsymbol{l}_s$ indicate the current element in primary coil 1, primary coil 2 and the secondary coil, respectively. $\boldsymbol{R}_i$ is the distance vector from the current element of primary coil *i* to the secondary coil's current element, and $\boldsymbol{R}_{12}$ is the distance vector from the current element of one primary coil to the other primary coil's current element.

TABLE I
SYSTEM PARAMETERS

Symbol	Note	Value
U_{in}	RMS source voltage	10V
f	Resonant frequency	100kHz
R_{in}	Source resistance	1Ω
R	Coil resistance	0.1Ω
R_L	Load resistance	10Ω

TABLE II
THE POSITION OF SECONDARY COIL AND CORRESPONDING VALUES OF x

Position of secondary coil(O')	x / cm
O	0
O_{p1}	-8
O_{p2}	8

IV. TOPOLOGICAL TRANSFORMATION AND HIERARCHICAL COMPENSATION CAPACITOR CONTROL

In order to determine the positions where $P_1 = P_2$ and to propose an accurate topological transformation as well as a hierarchical compensation capacitor control, the receiving power characteristics of the two topologies are analyzed by moving the secondary coil. Theoretical and experimental parameters are the same in this paper. The two independent primary coils on the primary side are set 0.01m away from each other. The side length of each coil is 0.15m and the number of turns is 7. The inductance of a single coil L and that of series connected coils L_{sum} are $21.4\mu H$ and $37.4\mu H$, respectively. According to (3) and (7), the compensation capacitor for systems with a single primary coil and two primary coils are $C_{p1} = 118.4nF$ and $C_{p2} = 135.5nF$, respectively. The other system parameters are presented in Table I.

In (4) and (8), the mutual inductances M_1 and M_2 change when secondary coil moves and can be calculated by

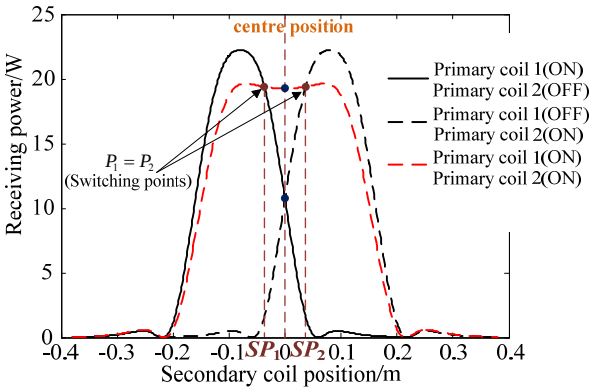

Fig. 7. Comparative characteristics curves of receiving power as a function of secondary coil position.

(10). With reference to Fig. 5, x is defined to represent the position of the secondary coil and the numerical values are derived and displayed in Table II.

As shown in Fig. 6, $\boldsymbol{R}_i$ is determined by x so that M_i can be calculated as a function of x when the other parameters are fixed. Specifically, the relationship between M_i and x can be obtained based on formula (10). The correlation between P_i and x can be further derived according to formula (4) and formula (8). For systems with a single primary coil topology and those with a two primary coil topology, the receiving power is calculated when x changes. The relationships between the receiving powers and location changes of the secondary coil are shown in Fig. 7. Systems with a single primary coil topology consist of two cases in which primary coil 1 or primary coil 2 is excited. Systems with a two primary coils topology refers to the case in which primary coil 1 and primary coil 2 are excited at the same time.

It is shown in Fig. 7 that $P_1 = P_2$ when $x = -4cm$ and $x = 4cm$. Therefore, without considering the moving speed of the secondary coil and the system response time, the switching points can be determined at $x = -4cm$ and $x = 4cm$. Taking the moving speed v(m/s) of the secondary coil and the system response time t(s) into consideration, the switching points should be ahead of vt(m) in the proposed control strategy. For instance, the moving speed is considered in reference [16]. A system with a response time of $300\mu s$ and a driving speed of 100km/h, should be turned on when the EV arrives at a position which is approximate 1cm away from the charging area. Since the control strategy can be adjusted according the criteria mentioned above for different driving speeds, the driving speed is not taken into account in the following studies. On the basis of the above characteristic analysis, the topological transformation and the hierarchical compensation capacitor control are proposed. When the secondary coil moves to $x = -4cm$, the primary circuit is transformed from a single coil topology to a two connected coil topology and the compensation capacitor is changed from $C_{p1} = 118.4nF$ to $C_{p2} = 135.5nF$. When the secondary coil moves to $x = 4cm$, the primary circuit is transformed from a two connected coil topology to a single coil topology and compensation capacitor is changed from $C_{p2} = 135.5nF$ to $C_{p1} = 118.4nF$. The distance ranging from O_{p1} to O_{p2} is defined as a cycle. The topological transformation and the hierarchical compensation capacitor control strategy of the cycle is illustrated in Table III.

TABLE III
TOPOLOGICAL TRANSFORMATION AND HIERARCHICAL COMPENSATION CAPACITOR CONTROL STRATEGY

Secondary coil position(O')	$O_{p1} \rightarrow SP_1$	$SP_1 \rightarrow SP_2$	$SP_2 \rightarrow O_{p2}$
x / cm	[-8,-4)	[-4,4)	[4,8)
State of primary coils	primary coil 1 (ON) primary coil 2 (OFF)	primary coil 1 (ON) primary coil 2 (ON)	primary coil 1 (OFF) primary coil 2 (ON)
Hierarchical compensation capacitor	118.4nF	135.5nF	118.4nF

With the proposed topological transformation of the primary circuit and the hierarchical compensation capacitor control, the large power fluctuation is avoided when the secondary coil moves under the condition of a fixed frequency. In addition, the receiving power in the middle positions of the two primary coils increases significantly.

V. EXPERIMENTAL VERIFICATION

In practice, on-road wireless charging power is at a high power rating reaching into the kW level. As a result, the start-up, stopping and conversion between different working conditions are no longer ideal processes in practical applications. Accordingly, the selection of electronic devices, the system response time, the voltage impact caused by the primary circuit transformation and the loss caused by the transformation switches should be taken into account. However, this paper intends to verify the correctness of the proposed system structure and control strategy applied to systems with different power levels. Thus, a size-reduced experimental prototype is designed.

To verify the correctness of the theoretical analysis, an experimental prototype is constructed, as shown in Fig. 8. The segmented primary coils and corresponding compensation capacitors are controlled by programmed switches. The control orders are sent by a micro-controller so that the coils and compensation capacitors can be controlled independently.

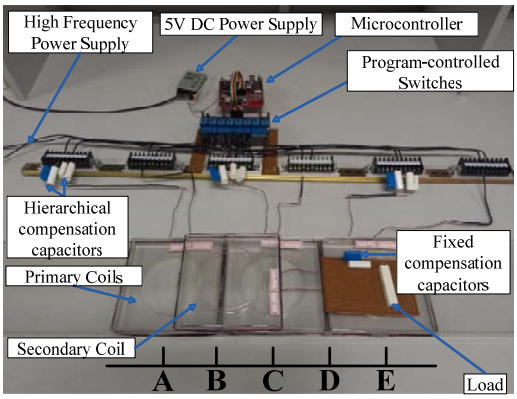

Fig. 8. Experimental prototype of segmented on-road charging system.

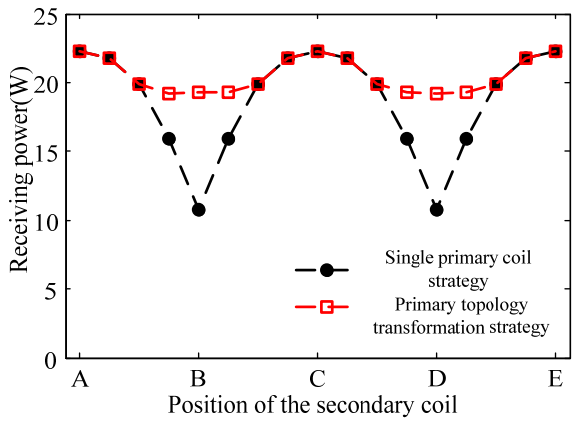

(a) Receiving power according to position variations of the secondary coil.

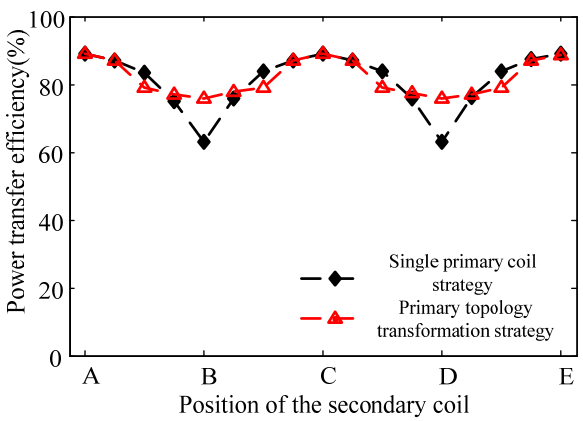

(b) Power transfer efficiency according to position variations of the secondary coil.

Fig. 9. Comparative experimental results of two strategies.

A typical system with a single primary coil topology and a system with the proposed topological transformation of the primary circuits as well as the hierarchical compensation capacitor control are comparatively analyzed. The parameters in the experimental section are identical to the above theoretical parameters. The voltage and frequency of the high frequency power supply are 10V and 100kHz, respectively. The load resistance is 10Ω. Side lengths of the primary coils

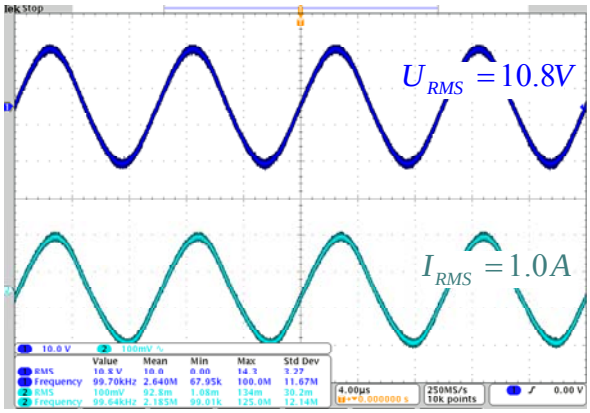

(a) Load voltage and current waveforms of system with single energized primary coil at a time.

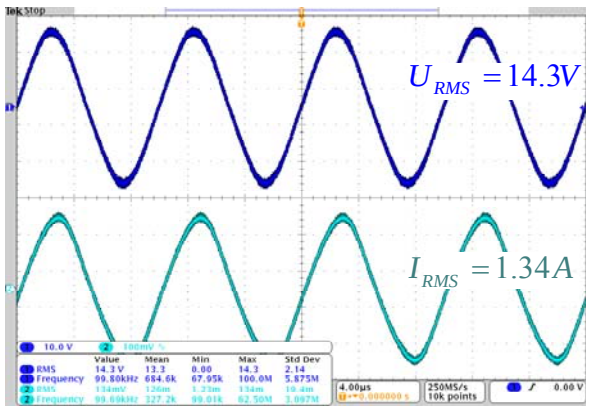

(b) Load voltage and current waveforms of system with proposed structure and strategy.

Fig. 10. Comparative measured results of load voltages and currents when secondary coil is in the middle position between two adjacent primary coils.

and the secondary coil are 0.15m. The vertical distance between the secondary coil and the primary coils is 0.04m. The secondary coil moves in the horizontal direction. The compensation capacitor used in the system with a single primary coil is $C_{p1}=118.4nF$. Only one primary coil is excited at any time and next one is turned on when the secondary coil moves to the middle position of the two primary coils. As for the proposed strategy, when the secondary coil moves to the position $x=-4cm$, primary coil 1 and primary coil 2 are excited at the same time. Meanwhile, the compensation capacitor is changed from $C_{p1}=118.4nF$ to $C_{p2}=135.5nF$. When the secondary coil moves to the position $x=4cm$, primary coil 1 is shut down and primary coil 2 continues to be powered. At the same time, the compensation capacitor is changed from $C_{p2}=135.5nF$ to $C_{p1}=118.4nF$. Applying the above control strategy when the secondary coil moves the distance of two cycles, the receiving power and the power transfer efficiency according to the position variations of the secondary coil are derived

and shown in Fig. 9(a) and Fig. 9(b), respectively.

It can be seen from Fig. 9(a) that the receiving power of the system with the proposed topological transformation of the primary circuit and the hierarchical compensation capacitor control remains in a high level. Compared with the system with a single primary coil topology, the receiving power of the proposed system in the middle position rises from 10.8W to 19.2W. Moreover, the power transfer efficiency is improved with the proposed control strategy when the secondary coil is in the middle position of the two adjacent primary coils as shown in Fig. 9(b). The voltages and currents are measured by an oscilloscope, voltage probe and current probe. It should be noted that the detection of the current is shown in the form of voltage, which can be converted by 1A/0.1V. Comparative measured results including load voltage waveforms and load current waveforms are shown in Fig. 10(a) and Fig. 10(b), respectively, when the secondary coil is placed in the middle position between the two primary coils. Fig. 10(a) represents the load voltage waveform and current waveform of a system with a single energized primary coil at a given time. Fig. 10(b) denotes the load voltage waveform and current waveform of a system with the proposed structure and strategy. The obtained experimental results demonstrate the correctness of the theoretical analysis.

VI. CONCLUSION

In order to solve the problem of on-road charging systems with a single energized primary coil, specifically the receiving power decline in the position between the two primary coils, a novel strategy for the topological transformation of the primary circuit and a hierarchical compensation capacitor control are introduced. Compared with systems with a single energized primary coil at any given time, the proposed structure and strategy achieve a more stable receiving power without frequency regulation. Meanwhile, according to experimental results, the receiving power in the position between the two primary coils is enhanced from 10.8W to 19.2W. Furthermore, the power transfer efficiency in the identical position is improved as well. The paper concentrated on the topological transformation of the primary circuit and the hierarchical compensation capacitor control. Nevertheless, a stable and efficient on-road charging system with segmented primary coils requires fast switching control and precise position detection, which are of great interest in this paper to improve the system performance. According to actual electrical vehicle applications with a high power rating, several issues including the losses caused by the transformation switches and the voltage impact caused by the primary circuit transformation should be taken into consideration in follow-up studies.

ACKNOWLEDGMENT

This work is financially supported by National Nature Science Youth Foundation of China (No. 51507032) and Nature Science Youth Foundation of Jiangsu Province (No. BK20150617).

REFERENCES

[1] S. Li and C. C. Mi, "Wireless Power Transfer for Electric Vehicle Applications," *IEEE J. Emerg. Sel. Topics Power Electron.*, Vol. 3, No. 1, pp. 4-17, Mar. 2015.

[2] F. Musavi and W. Eberle, "Overview of wireless power transfer technologies for electric vehicle battery charging," *IET Power Electron.*, Vol. 7, No. 1, pp. 60-66,Jan. 2014.

[3] G. Buja, M. Bertoluzzo, and K. N. Mude, "Design and Experimentation of WPT Charger for Electric City Car," *IEEE Trans. Ind. Electon.*, Vol.62, No. 12, pp. 7436-7447, Dec. 2015.

[4] C. Duan, C. G. Jiang, and A. Taylor, "Design of a zero-voltage-switching large-air-gap wireless charger with low electric stress for electric vehicles," *IET Power Electron.*, Vol. 6, No. 9, pp. 1742-1750, Jan. 2014.

[5] J. Y. Lee, H. Y. Shen, and K. W. Lee, "Design and implementation of weaving-type pad for contactless EV inductive charging system," *IET Power Electron.*, Vol. 7, No. 10, pp. 2533-2542, Oct. 2014.

[6] X. D. T. García, J. Vázquez, and P. Roncero-Sánchez, "Design, implementation issues and performance of an inductive power transfer system for electric vehicle chargers with series–series compensation," *IET Power Electron.*, Vol. 8, No. 10, pp. 1920-1930, Sep. 2015.

[7] S. Y. Choi, B. W. Gu, and S. Y. Jeong, "Advances in Wireless Power Transfer Systems for Roadway-Powered Electric Vehicles," *IEEE J. Emerg. Sel. Topics Power Electron.*, Vol. 3, No. 1, pp. 18-36, Mar. 2015.

[8] F. Sato, J. Murakami, and T. Suzuki, "Contactless energy transmission to mobile loads by CPLS-test driving of an EV with starter batteries," *IEEE Trans. Magn.*, Vol. 33, No. 5, pp. 4203-4205, Sep. 1997.

[9] G. A. Covic, J. T. Boys, and M. L. G. Kissin, "A Three-Phase Inductive Power Transfer System for Roadway-Powered Vehicles," *IEEE Trans. Ind. Electon.*, Vol. 54, No. 6, pp. 3370-3378, Dec. 2007.

[10] S. Y. Choi, S. Y. Jeong, and B. W. Gu, "Ultraslim S-Type Power Supply Rails for Roadway-Powered Electric Vehicles," *IEEE Trans. Power Electron.*, Vol. 30, No. 11, pp. 6456-6468, Nov. 2015.

[11] J. Hua, H. Z. Wang, Y. Zhao, and A. L. Zou, "LCL Resonant Compensation of Movable ICPT Systems with a Multi-load," *Journal of Power Electronics*, Vol. 15, No. 6, pp.1654-1663, Nov. 2015.

[12] S. Lee, B. Choi, and C. T. Rim, "Dynamics characterization of the inductive power transfer system for online electric vehicles by Laplace phasor transform," *IEEE Trans. Power Electron.*, Vol. 28, No. 12, pp. 5902-5909, Dec. 2013.

[13] S. Y. Choi, B. W. Gu, and S. W. Lee, "Generalized active EMF cancel methods for wireless electric vehicles," *IEEE Trans. Power Electron.*, Vol. 29, No. 11, pp. 5770-5783, Nov. 2014.

[14] M. Kim, H. Kim, and D. Kim, "A Three-phase wireless-power-transfer system for online electric vehicles with reduction of leakage magnetic fields," *Trans. Microw. Theory. Techn.*, Vol. 63, No. 11, pp. 3806-3813, Nov. 2015.

[15] G. R. Nagendra, L. Chen, and G. A. Covic, "Detection of

EVs on IPT highways," *IEEE J. Emerg. Sel. Topics Power Electron.*, Vol. 2, No. 3, pp. 584-597, Sep. 2014.
[16] H. Hao, G. A. Covic, and J. T. Boys, "An approximate dynamic model of LCL-T-based inductive power transfer power supplies," *IEEE Trans. Power Electron.*, Vol. 29, No. 10, pp. 5554-5567, Oct. 2014.
[17] K. Lee, Z. Pantic, and S. M. Lukic, "Reflexive field containment in dynamic inductive power transfer systems," *IEEE Trans. Power Electron.*, Vol. 29, No. 9, pp. 4592-4602, Sep. 2014.
[18] J. A. Russer, M. Dionigi, and M. Mongiardo, "A moving field inductive power transfer system for electric vehicles," in *Proc. European IEEE Microwave Conference (EuMC)*, pp. 519-522, 2013.
[19] J. M. Miller, O. Onar, and C. White, "Demonstrating dynamic wireless charging of an electric vehicle: The benefit of electrochemical capacitor smoothing," *IEEE Trans. Power Electron. Mag.*, Vol. 1, No. 1, pp. 12-24, Mar. 2014.
[20] J. M. Miller, P. T. Jones, and J. Li, "ORNL Experience and Challenges Facing Dynamic Wireless Power Charging of EV's," *IEEE Circuits Syst. Mag.*, Vol. 15, No. 2, pp. 40-53, May 2015.
[21] G. A. Covic and J. T. Boys, "Modern trends in inductive power transfer for transportation applications," *IEEE J. Emerg. Sel. Topics Power Electron.*, Vol. 1, No. 1, pp. 28-41, Mar. 2013.
[22] V. Prasanth, P. Bauer, "Study of misalignment for On Road Charging," in *Proc. IEEE Transportation Electrification Conference and Expo (ITEC)*, pp. 1-8, 2013.
[23] J. L. Villa, J. Sallan, J. F. Sanz Osorio, A. Llombart, "High-misalignment tolerant compensation topology for icpt systems," *IEEE Trans. Ind. Electron.*, Vol. 59, No. 2, pp. 945-951, Feb. 2012.
[24] J. Huh, S. W. Lee, W. Y. Lee, G. H. Cho, "Narrow-width inductive power transfer system for online electrical vehicles," *IEEE Trans. Power Electron.*, Vol. 26, No. 12, pp. 3666-3679, Dec. 2012.

Han Liu was born in Hubei, China, in 1993. He received his B.S. degree from the School of Electrical Engineering, Southeast University, Nanjing, China, in 2014, where he is presently working towards his Ph.D. degree. His current research interests include wireless power transfer technology, power electronics and EV dynamic wireless charging.

Linlin Tan received his B.S. degree in Electrical Engineering and Automation from Harbin Engineering University, Harbin, China, in 2008; and his Ph.D. degree in Electrical Engineering from Southeast University, Nanjing, China, in 2014. He is presently working as a Lecturer in the School of Electrical Engineering, Southeast University. Dr. Tan has published more than 20 papers. His current research interests include wireless power transfer, wireless charging for electric vehicles and wireless V2G.

Xueliang Huang received his B.S., M.S. and Ph.D. degrees in Electrical Engineering from Southeast University, Nanjing, China, in 1991, 1994 and 1997, respectively. From 2002 to 2004, he worked as a Post-Doctoral Fellow at the University of Tokyo, Tokyo, Japan. Since 2004, he has been a Professor in the Department of Electrical Engineering, Southeast University. He is the author of four books and more than 150 articles. He is also the creator of more than 40 inventions. His current research interests include wireless power transfer, the analysis of electromagnetic fields, and applied electromagnetic, intelligent electricity technology.

Jinpeng Guo received his B.S. degree in Electrical Engineering from the School of Electrical Engineering, Chongqing University, Chongqing, China, in 2014. He is presently working towards his M.S. degree in the School of Electrical Engineering, Southeast University, Nanjing, China. His current research interests include power electronics and their application in wireless power transfer systems.

Changxin Yan received his B.S. degree in Electrical Engineering from Jiangsu University, Zhenjiang, China, in 2010. He is presently working towards his M.S. degree in Electrical Engineering at Southeast University, Nanjing, China. His current research interests include wireless power transfer systems.

Wei Wang received his B.S. degree in Electrical Engineering and Automation from Jiangnan University, Wuxi, China, in 2007; and his M.S. degree in Electrical Engineering from Southeast University, Nanjing, China, in 2013, where he is presently working towards his Ph.D. degree in Electrical Engineering. His current research interests include numerical methods of electromagnetic field computation and novel wireless power transfer systems.